J Mater Sci: Mater Electron
DOI 10.1007/s10854-016-5180-3

Facile bottom-up growth of pyramidally textured ZnO:Al films by combined chemical bathing and DC sputtering deposition

Zhicheng Chen[1] · Ruiqin Tan[1] · Ye Yang[3] · Hua Xu[2] · Yuehui Lu[3] · Chaoting Zhu[3] · Weijie Song[3]

Received: 29 March 2016 / Accepted: 11 June 2016
© Springer Science+Business Media New York 2016

Abstract We developed a facile bottom-up approach to achieve the well-faceted pyramidally textured ZnO:Al (AZO) thin films on non-conductive glass substrates by combining chemical bathing and DC magnetron sputtering deposition. The chemical bathing deposition (CBD) was adopted to generate the ZnO nanorods (NRs) with a terminated plane of (001), followed by the further growth of (101)-faceted AZO pyramidal tips using DC sputtering. The structural, optical, and electrical properties of pyramidally textured AZO films were mainly governed by the size and distribution of ZnO NRs. When the length and the diameter of ZnO NRs were around 450 and 150 nm, respectively, controlled through the CBD process, the AZO film grown on the NRs showed a low resistivity of 9.7×10^{-4} Ω cm and a high average transmittance of 85.7 % at wavelengths of 400–1100 nm. The well-faceted pyramidal textures brought about a maximum haze value of 66.0 % at 355 nm and an average haze of 14.5 % at wavelengths of 355–1100 nm. This proposed simple strategy may benefit the studies on growth of pyramidally textured transparent conducting oxides on non-conductive substrates for high-efficient light harvesting through a low-cost and scalable process.

✉ Ruiqin Tan
tanruiqin@nbu.edu.cn

Hua Xu
xuhua@nbu.edu.cn

[1] Faculty of Electrical Engineering and Computer Science, Ningbo University, Ningbo 315211, People's Republic of China

[2] Department of Physics and Institute of Optics, Ningbo University, Ningbo 315211, People's Republic of China

[3] Ningbo Institute of Material Technology and Engineering, Chinese Academy of Sciences, Ningbo 315201, People's Republic of China

1 Introduction

Magnetron-sputtered ZnO:Al (AZO) films have been widely applied in thin film solar cells as front transparent conducting oxide (TCO) contact due to its excellent optical performance and electrical properties [1–4]. In order to increase the light absorption of thin film solar cells and harvest light efficiently [5–8], the surface of AZO films are generally textured, giving rise to a high haze value [9–12] and a sufficient light trapping [13, 14]. Unlike boron-doped ZnO (BZO) thin films grown using low-pressure chemical vapor deposition [15], the surface textured AZO films are often achieved by top-down chemical wet etching [16–18]. As a typical etching reagent, diluted hydrochloric (HCl) acid is used to endow the AZO films with "crater" surface structure [19–21]. However, the surface morphology and uniformity are strongly dependent on etching rate, crystal orientation in AZO films, and the resultant etching behavior [22–24]. The textured ZnO:Al (AZO) film with crater-like structure also has poor performance in light trapping comparing to those with pyramid-like structure [25]. So it would provide more degrees of freedom in surface texturing of AZO if there is a simple un-etching and bottom-up growth approach. In fact, it is still a challenge to achieve the well-faceted pyramidal AZO films [26]. Under peculiar conditions (e.g., ionic liquids, RF magnetron sputtering in a mixed gas at a high temperature of 400 °C [27, 28]), ZnO with a hexagonal pyramidal structure could be prepared. Recently, Shinagawa et al. [29] prepared the high-haze ZnO films with a hexagonal pyramidal structure composed of (101) and (001) planes on

Published online: 18 June 2016

www.spm.com.cn

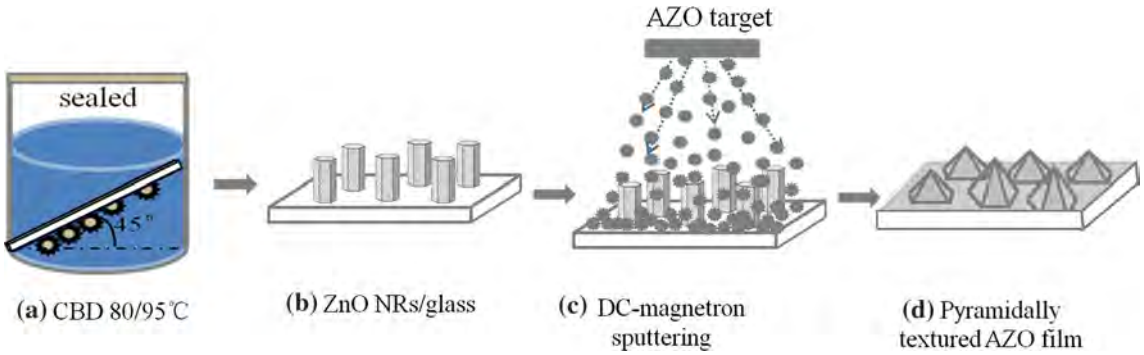

Fig. 1 Schematic illustration of the bottom-up growth of pyramidally textured AZO films

F-doped SnO_2 substrates by electrodeposition without special treatment and realized high-efficient light trapping in ZnO/Cu_2O thin-film solar cells. In principle, AZO, as a ZnO-based TCO, should have much in common with the pyramidal ZnO growth in terms of growth kinetics and thermodynamics. The understanding of the growth mechanism of hexagonal pyramidal tips on the ZnO films might inspire the formation of pyramidally textured AZO films.

In this work, we reported a facile bottom-up approach to form the well-faceted pyramidal texture in AZO thin films on ordinary non-conductive glass substrates by a combined chemical bathing and direct-current (DC) magnetron sputtering technique. The process consisted of two steps. Firstly, the hexagonal ZnO nanorods (NRs) with a terminated plane of (001) were prepared by chemical bathing deposition (CBD). Then the (101)-faceted AZO was sputtered onto the ZnO NRs to generate the pyramidal tips eventually. The structural, optical, and electrical properties of the prepared AZO films were investigated, which demonstrated a well-faceted pyramidal structure, a low resistivity of 9.7×10^{-4} Ω·cm, and a high average transmittance of 85.7 % at wavelengths from 400 to 1100 nm without loss of haze (e.g., a maximum haze value of 66.0 % at 355 nm). The proposed method has no need for specific substrates and peculiar conditions, which is promising for high-efficient light harvesting as TCO electrodes in thin film solar cells.

2 Experimental

The cleaned low-iron glasses ($100 \times 100 \times 3.2$ mm^3) were chosen as substrates. The ZnO NRs were prepared by a typical CBD process [30] which was composed of two steps, namely seeding and growth. The ZnO nanocrystal seeding was performed at 450 °C on glass substrates by thermally decomposing the zinc acetate ($Zn(CH_3COO)_2$·$2H_2O$) precursor dissolved in ethanol (C_2H_5OH, EtOH) with a concentration of 0.01 M. During the NRs growth, the coated glass substrates with seeds were immersed in an aqueous solution containing equal molar concentrations of 0.025 M zinc nitrate hexahydrate ($Zn(NO_3).6H_2O$) and hexamethylenetetramine (HMT, $C_6H_{12}N_4$). In our experiments, the growth was carried out at the temperatures of 80 °C for 0.5, 1.5 h, and 95 °C for 2.0 h, denoted as $C_{80–0.5}$, $C_{80–1.5}$, and $C_{95–2.0}$, respectively.

The AZO films were then deposited on the ZnO NRs by DC magnetron sputtering using a home-made 2 wt% AZO ceramic target (98 wt% ZnO + 2 wt% Al_2O_3) [31], named as F–$C_{80–0.5}$, F–$C_{80–1.5}$, and F–$C_{95–2.0}$. The distance between the target and substrate was fixed at 90 mm. The base pressure in the chamber was kept below 4×10^{-4} Pa and the sputtering pressure was 0.6 Pa. The sputtering process was carried out at a substrate temperature of 350 °C and a sputtering DC power of 100 W in pure Ar atmosphere. The deposition time was determined to be 25 min for all the samples, which was determined by the deposition rate of AZO films, 16 nm/min, on bare glass substrates. The whole process composed of the preparation of ZnO NRs and the deposition of AZO to form the pyramidal texture was illustrated in Fig. 1. For comparison, the control sample was also fabricated on the bare glass substrate under the same sputtering conditions, named as F–NC.

The structural properties of the as-deposited samples were analyzed by an X-ray diffraction (XRD, Bruker AXS D8 Advance, USA) with Cu K_α radiation ($\lambda = 1.5406$ Å).The surface morphology was characterized by a scanning electron microscope (SEM, Hitachi S4800, JP) and an atomic force microscope (AFM, CSPM5500,CHN). The optical transmittance and haze value of the films on the substrates were measured using a UV/visible/NIR spectrophotometer (Perkin-Elmer, Lambda 950, USA). The resistivity, carrier concentration, and mobility were measured using the Van der Pauw method by Hall measurements (Accent, HL5500PC, UK).

3 Results and discussion

Figure 2a–c shows the SEM images of ZnO NRs prepared by CBD at the various temperatures and time. Though there are some differences for the samples in terms of

www.scm.com.cn

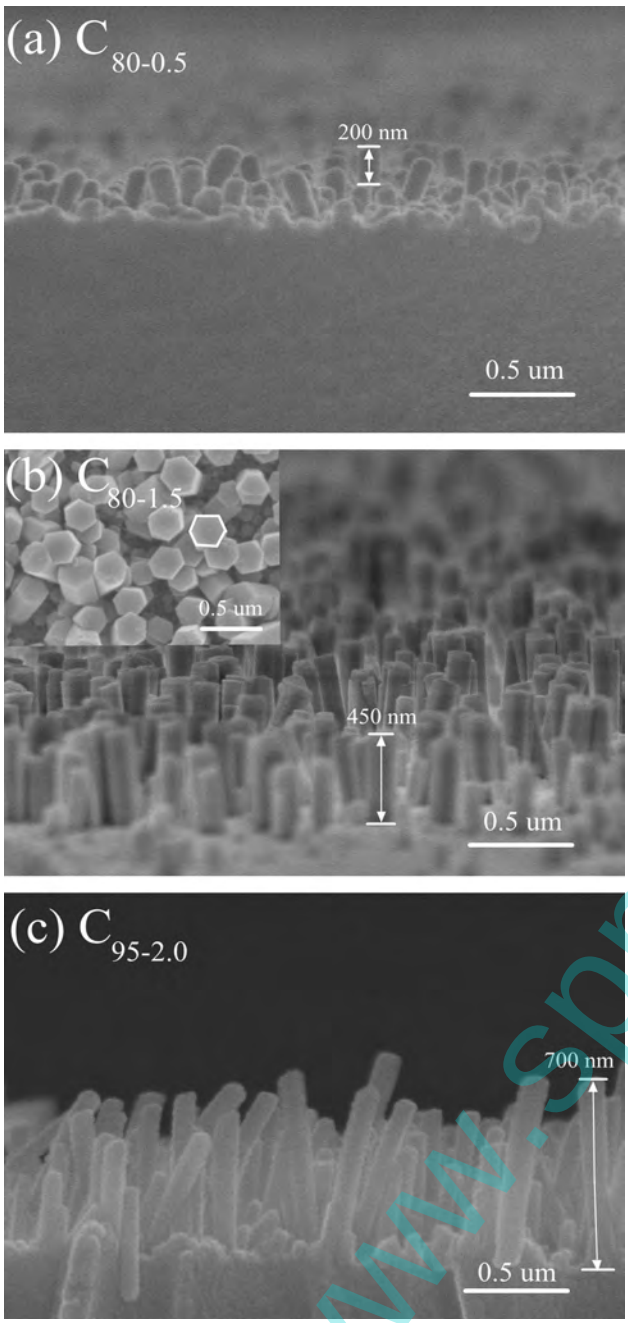

Fig. 2 Cross-sectional SEM images of the ZnO NRs, **a** $C_{80–0.5}$, **b** $C_{80–1.5}$, and **c** $C_{95–2.0}$, which were prepared by CBD at the different temperatures and time. Inset: the top-view of Sample $C_{80–1.5}$. The hexagonal plane was marked by the white line, which was considered as the exposed (001) plane

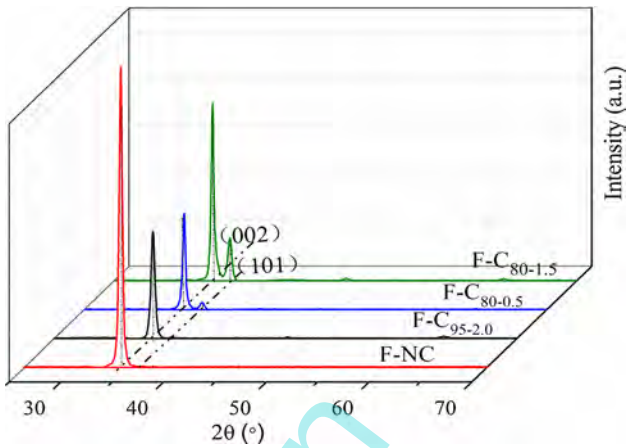

Fig. 3 XRD patterns of the AZO films grown on the different ZnO NRs

uniformity and orientation, all of them prominently exhibited the cylindrical structure. The best hexagonal cylindrical structure was observed from Sample $C_{80–1.5}$, as shown in Inset of Fig. 2b. The length and diameter of ZnO NRs were strongly dependent on the temperature and time of CBD. For Sample $C_{80–0.5}$, the average length of 200 nm and diameter of 120 nm were obtained under the relatively low temperature (80 °C) and short time (0.5 h) of CBD. When the CBD time was increased to 1.5 h at the same temperature (i.e., Sample $C_{80–1.5}$), the longer ZnO NRs with the length of 450 nm were obtained and the diameter also became a little larger, around 150 nm. If increasing the CBD temperature and time simultaneously to 95 °C and 2.0 h, respectively (i.e., Sample $C_{95–2.0}$), the average length became larger (about 700 nm), while the diameter was smaller (about 50 nm). The results revealed that the size of ZnO NRs could be easily tailored by varying the CBD temperature and time.

Once the AZO films were deposited by DC magnetron sputtering onto the different ZnO NRs, it is of great interest that the pronounced (101) diffraction peak appeared in Samples $C_{80–0.5}$ and $C_{80–1.5}$, as shown in Fig. 3, except that the (002) diffraction peak presented in all the samples as an indication of a c-axis preferred orientation. The diffraction intensity of the (101) peak became larger with increasing the diameter of ZnO NRs, which was considered as an origin of the formation of pyramidally textured AZO films [27]. In addition, Samples F–$C_{80–1.5}$, F–$C_{80–0.5}$, and F–$C_{95–2.0}$ showed a smaller (002) peak intensity than that of Sample F–NC. And F–$C_{80–1.5}$, F–$C_{80–0.5}$, and F–$C_{95–2.0}$ showed an increase in full width at half maximum (FWHM) from 0.31° to 0.41° in, which was larger than that of Sample F–NC, only 0.21°. It implied that Sample F–$C_{80–1.5}$ had the highest crystallinity among the pyramidally textured AZO films though the crystallinity of AZO films grown on ZnO NRs (i.e., F–$C_{80–1.5}$, F–$C_{80–0.5}$, and F–$C_{95–2.0}$) was inferior to the control sample F–NC.

The surface morphology characterization further confirmed the appearance of pyramidal texture in AZO films grown on ZnO NRs. As shown in Fig. 4a–c, the pyramidal tips could be easily observed, while it was not the case in Fig. 4d. Obviously, the ZnO NRs were crucial to the

www.spm.com.cn

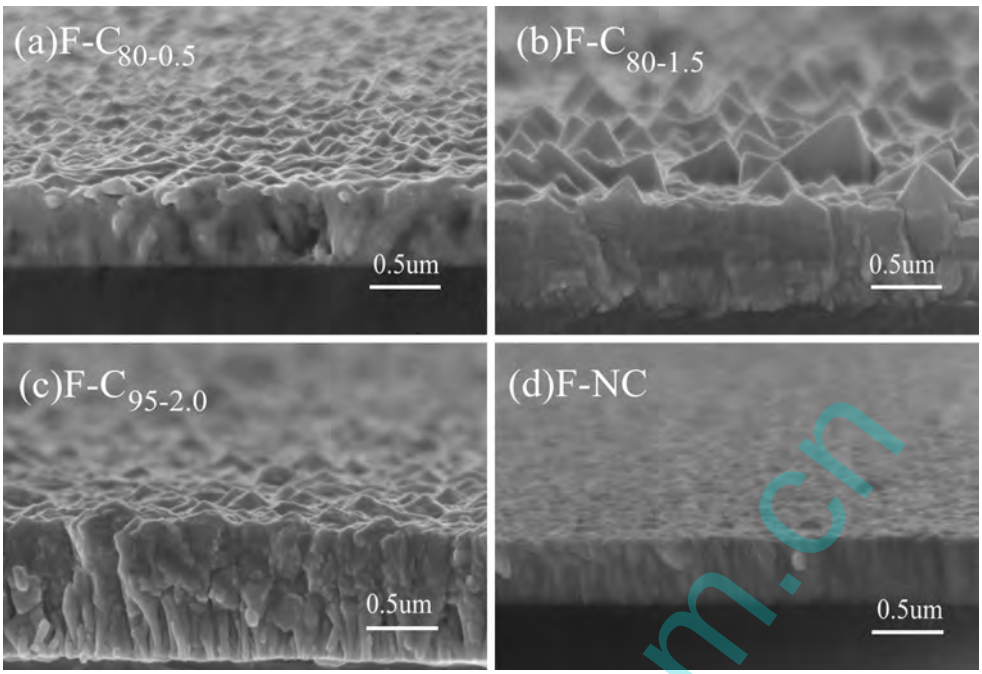

Fig. 4 Cross-sectional SEM images of the AZO films: **a** F–$C_{80–0.5}$, **b** F–$C_{80–1.5}$, **c** F–$C_{95–2.0}$, and **d** F–NC

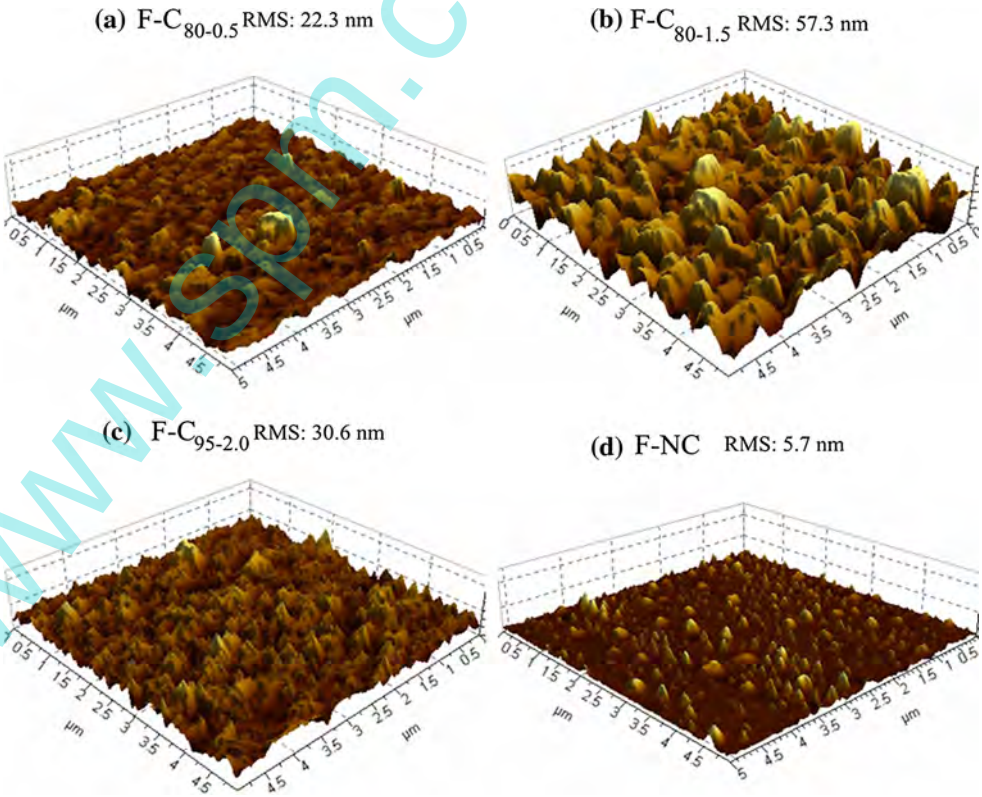

Fig. 5 3D AFM images of the AZO films with the roughness values: **a** F–$C_{80–0.5}$, **b** F–$C_{80–1.5}$, **c** F–$C_{95–2.0}$, and **d** F–NC

appearance of (101) plane and the resultant pyramidal texture in AZO thin films. During crystal growth, the polar surfaces generally appear as growing surface due to their high surface energy, making these facets small or even disappeared [27]. Since the surface energy of the (101) polar facets are higher than that of non-polar (100) facets,

www.spm.com.cn

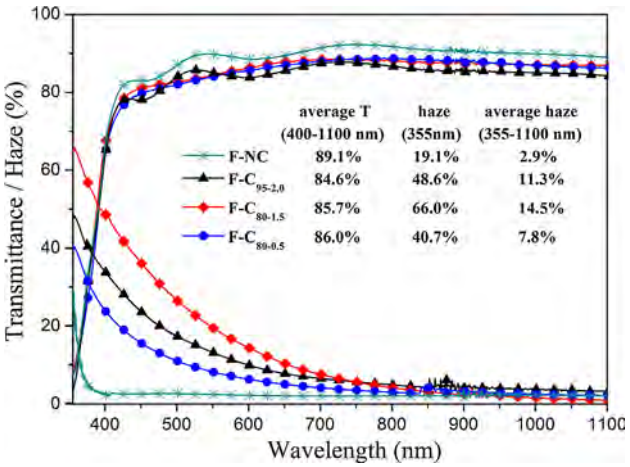

Fig. 6 Transmittance and haze spectra of the AZO films grown on the different ZnO NRs

the (101) polar facets usually grow too fast to be observed and they are unfavorable to be the exposed surfaces. In our experiment, it was believed that the appearance of (101) plane might be associated with the discretely distributed ZnO NRs on glass substrates, which affected the surface energy significantly. Therefore, the variation of surface energy was considered as one of the important reasons for the change of AZO growth behavior and the resultant formation of (101)-faceted pyramid tips. On the other hand, Fig. 5 shows that Samples F–$C_{80–1.5}$ had the highest root-mean-square (RMS) average roughness, 57.3 nm, implying the biggest pyramidal structures. It was in a good agreement with the highest (101) diffraction intensity of F–$C_{80–1.5}$ as an indication of pyramidal texture formation, as shown in Fig. 3. In addition, the thickness of Sample F–$C_{95–2.0}$ about (729 ± 30) nm was much larger than that of Samples F–$C_{80–0.5}$ (417 ± 22) nm, F–$C_{80–1.5}$ (458 ± 22) nm, and F–NC (406 ± 5) nm. The largest thickness in Sample F–$C_{95–2.0}$ might be associated with the shielding effects resulting from its large length underneath ZnO NRs during AZO sputtering. Meanwhile, the ion bombardment etching played few roles in Sample F–$C_{95–2.0}$ due to its small diameter.

Table 1 Results of the Hall measurements of the AZO thin films

Sample	Thickness (nm)	Resistivity (10^{-4} Ω cm)	Carrier concentration (10^{20} m^{-3})	Mobility (cm^2/Vs)
F–$C_{80–0.5}$	417 ± 22	9.4	3.4	19.3
F–$C_{80–1.5}$	458 ± 22	9.7	3.3	18.5
F–$C_{95–2.0}$	729 ± 30	14.0	2.6	16.8
F–NC	406 ± 5	7.8	3.7	21.6

Figure 6 shows the optical properties of Samples F–$C_{80–0.5}$, F–$C_{80–1.5}$, F–$C_{95–2.0}$, and F–NC. Except F–$C_{95–2.0}$, all the samples had the average transmittance above 85.0 % at wavelengths of 400–1000 nm. The relatively low transmittance in F–$C_{95–2.0}$ was associated with its large thickness compared with that of Samples F–$C_{80–0.5}$ and F–$C_{80–1.5}$. Interestingly, Samples F–$C_{80–0.5}$, F–$C_{80–1.5}$, and F–$C_{95–2.0}$ with pyramid texture structure showed a high haze value compared with that of the control sample F–NC. Importantly, Sample F–$C_{80–1.5}$ grown on the ZnO NRs with the largest diameter demonstrated the highest haze in terms of both maximum and average values, which further confirmed the roles of (101)-polar facets in pyramidal texture formation. The maximum and average haze values of Sample $C_{80–1.5}$ reached 66.0 % at 355 nm and 14.5 % at wavelengths of 355–1100 nm. It would greatly benefit light harvesting of solar cells in the visible and near-IR spectral ranges.

Table 1 shows the electrical properties of F–$C_{80–0.5}$, F–$C_{80–1.5}$, F–$C_{95–2.0}$, and F–NC. It found that the electric properties were associated with the structural properties of ZnO NRs. The control sample F–NC showed the lowest resistivity, the highest carrier concentration and the Hall mobility, which completely depended on the AZO film itself with few influences from substrates. For F–$C_{80–0.5}$, F–$C_{80–1.5}$, and F–$C_{95–2.0}$, with the increase of ZnO NRs length from 200 to 700 nm, the carrier concentration and the Hall mobility decreased from 3.4 × 10^{20} $cm^{-3}$and 19.3 cm^2/Vs to 2.6 × 10^{20} cm^{-3} and 16.8 cm^2/Vs, respectively, and the resistivity increased from 9.4 × 10^{-4} to 1.4 × 10^{-3} Ω cm, which were ascribed to the various crystallinity and densification [32, 33]. Therefore, it could be concluded that the large diameter in ZnO NRs was beneficial to light harvesting due to high transmittance and haze without much loss of electrical properties. The pyramidally textured AZO films could be further optimized by tailoring the ZnO NRs growth.

4 Conclusions

In this study, a facile bottom-up approach was developed to prepare the well-faceted pyramidally textured AZO thin films on ordinary substrates. A combination of CBD and DC-magnetron sputtering was used to obtain ZnO NRs with a terminated plane of (001) and the (101)-faceted AZO pyramidal tips on the NRs, respectively. The influences of ZnO NRs with different length and diameter on the structural, optical and electrical properties of the AZO films were investigated. It was found that Sample $C_{80–1.5}$ had the highest RMS roughness of 57.3 nm, one order of

www.spm.com.cn

magnitude larger than that of the control sample grown on bare glass substrate. The average transmittance of it was 85.7 % at wavelengths of 400–1000 nm and the maximum haze value was 66.0 % at 355 nm. It exhibited the carrier concentration, Hall mobility, and resistivity of 3.3×10^{20} cm^{-3}, 18.5 cm^2/Vs, and 9.7×10^{-4} Ω cm, respectively, which was comparable with the control sample F–NC. This work revealed that the combined method of magnetron sputtering and CBD was able to achieve pyramidally textured AZO thin films on non-conductive substrates with satisfactory optical and electrical properties, which was of great significance for high-efficient light harvesting in photovoltaic devices through a low-cost and scalable process.

Acknowledgments This work is supported by the National Science Foundation of China (Nos. 21377063, 61275114) and K. C. Wong Magna Fund in Ningbo University.

References

1. M. Berginski, J. Hupkes, M. Schulte, G. Schöpe, H. Stiebig, B. Rech, M. Wuttig, J. Appl. Phys. **101**, 074903 (2007)
2. R. Menner, D. Hariskos, V. Linss, M. Powalla, Thin Solid Films **519**, 7541 (2011)
3. H. Zhu, J. Hupkes, E. Bunte, J. Owen, S.M. Huang, Sol. Energy Mater. Sol. Cells **95**, 964 (2011)
4. K. Zhu, Y. Yang, T. Wei, R. Tan, P. Cui, W. Song, K.L. Choy, J. Mater. Sci. Mater. Electron. **24**, 3844 (2013)
5. M. Theuring, M. Vehse, K. von Maydell, C. Agert, Thin Solid Films **558**, 294 (2014)
6. P. Chen, G. Hu, Q.H. Wang, Appl. Phys. Lett. **105**, 073506 (2014)
7. V.A. Antohe, M. Mickan, F. Henry, R. Delamare, L. Gence, L. Piraux, Appl. Surf. Sci. **313**, 607 (2014)
8. A. Bai, Y. Tang, J. Chen, Chem. Phys. Lett. **636**, 134 (2015)
9. M. Wang, S. Li, P. Zhang, Y. Wang, H. Li, Z. Chen, Chem. Phys. Lett. **639**, 283 (2015)
10. P. Buehlmann, J. Bailat, D. Domine, A. Billet, F. Meillaud, A. Feltrin, C. Ballif, Appl. Phys. Lett. **91**, 143505 (2007)
11. D. Domine, P. Buehlmann, J. Bailat, A. Billet, A. Feltrin, C. Ballif, Phys. Status Solidi RRL **2**, 163 (2008)
12. S. Nicolay, M. Despeisse, F.J. Haug, C. Ballif, Sol. Energy Mater. Sol. Cells **95**, 1031 (2011)
13. J. Meier, J. Spitznagel, U. Kroll, C. Bucher, S. Fay, T. Moriarty, A. Shah, Thin Solid Films **451**, 518 (2004)
14. S. Fernandez, O. De Abril, F.B. Naranjo, J.J. Gandia, Thin Solid Films **520**, 4144 (2012)
15. M.L. Addonizio, L. Fusco, J. Alloy. Compd. **622**, 851 (2015)
16. S. Kim, J.W. Chung, H. Lee, J. Park, Y. Heo, H.M. Lee, Sol. Energy Mater. Sol. Cells **119**, 26 (2013)
17. Y. Wang, X. Zhang, L. Bai, Q. Huang, C. Wei, Y. Zhao, Appl. Phys. Lett. **100**, 263508 (2012)
18. S.J. Tark, M.G. Kang, S. Park, J.H. Jang, J.C. Lee, W.M. Kim, J.S. Lee, D. Kim, Curr. Appl. Phys. **9**, 1318 (2009)
19. S. Fernandez, O. De Abril, F.B. Naranjo, J.J. Gandia, Sol. Energy Mater. Sol. Cells **95**, 2281 (2011)
20. X. Yan, S. Venkataraj, A.G. Aberle, Int. J. Photoenergy **2015**, 1 (2015)
21. H. Zhu, J. Hupkes, E. Bunte, S.M. Huang, Appl. Surf. Sci. **261**, 268 (2012)
22. J.N. Ding, F. Ye, N.Y. Yuan, C.B. Tan, Y.Y. Zhu, G.Q. Ding, Z.H. Chen, Appl. Surf. Sci. **257**, 1420 (2010)
23. Z.L. Wang, Mat. Sci. Eng. R. **64**, 33 (2009)
24. M. Law, L.E. Greene, J.C. Johnson, R. Saykally, P. Yang, Nat. Mater. **4**, 455 (2005)
25. Y.H. Hu, Y.C. Chen, H.J. Xu et al., Engineering **02**, 12 (2010)
26. D. Wan, F. Huang, Y. Wang, A.C.S. Appl, Mater. Interfaces. **2**, 2147 (2010)
27. X. Zhou, Z.X. Xie, Z.Y. Jiang, Q. Kuang, S.H. Zhang, T. Xu, R.B. Huang, L.S. Zheng, Chem. Commun. **44**, 5572 (2005)
28. Y.H. Liang, J.H. Huang, N.C. Chang, C.P. Liu, Cryst. Growth Des. **9**, 2021 (2009)
29. T. Shinagawa, K. Shibata, O. Shimomura, M. Chigane, R. Nomura, M. Izaki, J. Mater. Chem. C **2**, 2908 (2014)
30. N.J. Ridha, H. Jumali, M. Hafizuddin, A.A. Umar, F. Alosfur, Int. J. Electrochem. Sci. **8**, 4583 (2013)
31. Y.L. Zhang, Y. Yang, J.H. Zhao, R.Q. Tan, P. Cui, W.J. Song, J. Sol-Gel. Sci. Technol. **51**, 198 (2009)
32. H. Zeng, G. Duan, Y. Li, S. Yang, X. Xu, W. Cai, Adv. Funct. Mater. **20**, 561 (2010)
33. M. Wang, Y. Yang, P. Lan, K. Zhu, Q. Huan, Y. Lu, R. Tan, W. Song, Phys. Status Solidi RRL **8**, 172 (2014)

www.spm.com.cn